



## Optimization of spray drying microencapsulation of olive pomace polyphenols using Response Surface Methodology and Artificial Neural Network



Bahar Aliakbarian<sup>a,b</sup>, Fábio Coelho Sampaio<sup>c</sup>, Janaína Teles de Faria<sup>d</sup>, Cristiano Grijó Pitangui<sup>e</sup>, Francesca Lovaglio<sup>a</sup>, Alessandro Alberto Casazza<sup>a</sup>, Attilio Converti<sup>a,\*</sup>, Patrizia Perego<sup>a</sup>

<sup>a</sup> Department of Civil, Chemical and Environmental Engineering, University of Genoa, Via Opera Pia 15, 16145 Genoa, Italy

<sup>b</sup> Department of Supply Chain Management, Michigan State University, East Lansing, MI, United States

<sup>c</sup> Department of Microbiology, Federal University of Viçosa, Avenida PH Rolfs, s/n, Campus Universitário, 36570-000, Viçosa, Minas Gerais, Brazil

<sup>d</sup> Agricultural Sciences Institute, Federal University of Minas Gerais, Avenida Universitária, 1000, Bairro Universitário, 39400-000 Montes Claros, Minas Gerais, Brazil

<sup>e</sup> Department of Technology and Civil Engineering, Computation, Humanities, Federal University of São João del-Rey, Campus Alto Paraopeba, Rod. MG 443 - km 7, 36420-000 Ouro Branco, Minas Gerais, Brazil

### ARTICLE INFO

#### Keywords:

Antioxidant activity  
Experimental design  
Statistic models  
Moisture content  
Water solubility

### ABSTRACT

This study was performed to determine the optimum conditions for spray drying microencapsulation of olive pomace extract, in order to stabilize its phenolic compounds using maltodextrin as carrier material. To this purpose, a comparison optimization study was performed using Response Surface Methodology or Artificial Neural Network, which revealed better prediction accuracy of the former. Maltodextrin concentrations (100–500 g/L), inlet-drying air temperatures (130–160 °C), feed flowrates (5.0–10.0 mL/min), and drying compressed air flowrates (20–32 m<sup>3</sup> h<sup>-1</sup>) were tested as the independent variables according to a Central Composite Face Centered design, and the results of microencapsulation yield, moisture content, water solubility, specific total polyphenol content, specific antioxidant activity and encapsulation efficiency were elaborated. Under optimal conditions, these responses varied in the ranges 65–82%, 9–14 g/100 g, 64–65%, 38–52 mg<sub>CAE</sub> g<sub>DM</sub><sup>-1</sup>, 230–487 μg<sub>Trolox</sub> g<sub>DM</sub><sup>-1</sup> and 85–92%, respectively. The same optimization regions for operative parameters were obtained using Response Surface Methodology or Artificial Neural Network. The results demonstrated that maltodextrin-based microcapsules containing olive pomace extract can effectively be produced by spray drying with good stability under storage conditions, and suggest that their remarkable antioxidant activity may be exploited to improve the properties of functional foods or pharmaceutical products.

### 1. Introduction

Olive oil industry produces a large amount of residues (Barbanera et al., 2016) causing serious environmental problems, particularly in the Mediterranean area. However, these residues can gain added value in a clean way, if exploited in different processes with economic and environmental benefits (Christoforou & Fokaides, 2016).

The three-phase centrifugation olive oil process generates a solid residue named olive pomace or husk and a liquid wastewater (Kalogeropoulos, Kaliora, Artemiou, & Giogios, 2014). Olive pomace, whose chemical composition depends on various factors such as olive variety, cultivation conditions and extraction method (Christoforou & Fokaides, 2016), has successfully been used, among other things, for phenolic compounds extraction (Aliakbarian, Casazza, & Perego, 2011;

Paini et al., 2015).

Owing to bioactive properties of olive pomace polyphenols (Aliakbarian, Palmieri, Casazza, Palombo, & Perego, 2012), such a by-product has alternatively been considered a promising source of antioxidants for pharmaceutical and food industries (Paini et al., 2015). Klen, Wondra, Vrhovšek, & Vodopivec (2015) divided olive pomace phenols into four classes: simple phenols such as tyrosol and its derivatives, cinnamic acids such as *p*-coumaric acid and verbascoside, flavonoids as rutin and apigenin, and secoiridoids as oleuropein and its derivatives.

Microencapsulation can be thought as an interesting alternative to stabilize olive pomace phenolics (Paini et al., 2015). This process consists of closing the active agent in a carrier (matrix) to protect it from light, oxygen, water or other environmental factors, increasing its

\* Corresponding author.

E-mail address: [converti@unige.it](mailto:converti@unige.it) (A. Converti).

shelf-life and promoting its controlled release (Poshadri & Aparna, 2010; Zhang, Li, Liu, & Zhang, 2015).

Spray drying is preferred over other techniques because it is cheaper, more flexible and can be easily operated and controlled (Desai & Park, 2005; Hojjati, Razavi, Rezaei, & Gilani, 2011). Its main steps are dispersion preparation and homogenization, atomization of the feed dispersion, and dehydration of atomized particles (Poshadri & Aparna, 2010; Zuidam & Shimoni, 2010). The final product quality and powder efficiency depend on the operating conditions such as inlet and outlet air temperatures, feed and air flowrates, atomization pressure and feed-to-carrier ratio (Zuidam & Shimoni, 2010). Maltodextrins, which are odor-, color- and tasteless carbohydrates with variable molecular weight, are widely used in cosmetic, food and pharmaceutical sectors and appear to be the best option as encapsulating agent in spray drying (Castro, Durrieu, Raynaud, & Rouilly, 2016). They have recently been used with success to microencapsulate anthocyanins (Akhavan Mahdavi, Jafari, Assadpoor, & Dehnad, 2016), oleoresin (Edris, Kalemba, Adamiec, & Piątkowski, 2016), phenolics from olive pomace (Paini et al., 2015) and procyanidins from hawthorn bark (Wyspiańska, Kucharska, Sokół-Łętowska, & Kolniak-Ostek, 2016), among others.

The objective of the present work was the microencapsulation of phenolic compounds from olive pomace extract by spray drying using maltodextrin as wall material. Following a previous study (Paini et al., 2015), this work was performed selecting wider ranges of spray drying operating conditions to optimize the process using both Response Surface Methodology (RSM) and Artificial Neural Network (ANN). The results of optimization using either statistical approach were then compared. The reason of selecting and comparing these two approaches is that RSM has been widely used for optimization of operative parameters in various processes (Aliakbarian, De Faveri, Converti, & Perego, 2008; Casazza, Aliakbarian, De Faveri, Fiori, & Perego, 2012; Gabbay Alves et al., 2017), while ANN is considered a powerful tool with higher accuracy and flexibility for modeling of experimental data of several biochemical processes when compared to RSM (Sampaio et al., 2016; Huang, Kuo, Chen, Liu, & Shieh, 2017). In this work, we investigated the effects of inlet-drying temperature, feed flowrate, compressed air flowrate and maltodextrin concentration on six responses, namely microencapsulation yield and efficiency, microcapsules moisture content, water solubility, specific total polyphenols content and specific antioxidant activity.

## 2. Materials and methods

### 2.1. Materials

Olive pomace (Taggiasca cultivar) was supplied by an Italian olive oil producer (Raineri S.p.A., Chiusanico, Italy). Methanol, acetic acid, ethanol, *n*-hexane, acetonitrile, maltodextrin (MD) (Dextrose Equivalent = 16.5–19.5), Folin–Ciocalteu reagent, 6-hydroxy-2,5,7,8-tetramethylchroman-2-carboxylic acid (Trolox), 2,29-azinobis (3-ethylbenzothiazoline-6-sulfonic acid) diammonium salt (ABTS), potassium persulfate, sodium carbonate and polyphenols standards (apigenin, caffeic acid, ferulic acid, catechin, tyrosol, hydroxytyrosol, oleuropein, protocatechuic, *p*-coumaric, syringic, vanillic acids and vanillin) were supplied by Sigma-Aldrich (St. Louis, MO, USA).

### 2.2. Extraction of polyphenols from olive pomace

Olive pomace stored at  $-20^{\circ}\text{C}$  was defrosted at room temperature ( $22 \pm 1^{\circ}\text{C}$ ), washed with *n*-hexane and extracted according to Aliakbarian et al. (2011) and Paini et al. (2016) with modifications. Briefly, extraction was carried out in a mixed high pressure-high temperature reactor, model 4560 (PARR Instrument, Moline, IL, USA), using a 1:1 (mL/mL) ethanol/deionized water solution. Extracts were centrifuged at 6000g for 10 min (model PK131, ALC, Alberta, Canada), maintained at  $4^{\circ}\text{C}$  for 24–48 h and filtered through membranes with

**Table 1**

Independent variables and their ranges used to microencapsulate the olive pomace extract by spray drying according to the Central Composite Face Centered design.

Independent variable	Unit	Symbol	Coded and actual levels		
			−1	0	+1
Inlet temperature (IT)	$^{\circ}\text{C}$	$x_1$	130	145	160
Maltodextrin concentration (MD)	g/L	$x_2$	100	300	500
Feed flowrate (FF)	mL/min	$x_3$	5.0	7.5	10.0
Air flowrate (AF)	$\text{m}^3/\text{h}$	$x_4$	20	26	32

12–15  $\mu\text{m}$ -pore diameter (Sartorius, Goettingen, Germany). Dry weight content of olive pomace extract (OPE) was determined drying it at  $105^{\circ}\text{C}$  up to constant weight. The extract was then stored at  $4^{\circ}\text{C}$ , protected from light and submitted to total polyphenols (TP) stability tests prior to experiments.

### 2.3. Microcapsule preparation

OPE microencapsulation was performed by spray drying as described by Paini et al. (2015) with modifications. Briefly, 50 mL of extract were mixed at room temperature with MD at three different concentrations (100, 300 and 500 g/L) and homogenized under magnetic stirring for 25–30 min. The resulting solution was fed to a mini spray dryer B290 (Büchi, Flawil, Switzerland) varying inlet-drying air temperature (IT), feed flowrate (FF) and compressed air flowrate (AF) according to Table 1. Compressed air at 3 bar was used to supply dry free-air at a 473 L/h flowrate (Q-Flow indicator, Vögtlin Instruments, Aesch, Switzerland), and the nozzle cleaner was set at 4. Resulting powders were weighed and kept at  $4^{\circ}\text{C}$  in closed vessels protected from light. Microencapsulation yield ( $Y_M$ , %) was calculated according to the equation (Paini et al., 2015):

$$Y_M = \frac{DW_M}{DW_E + W_{MD}} \times 100 \quad (1)$$

where  $DW_M$  (g) is total dry mass of recovered microcapsules,  $DW_E$  ( $1.4 \pm 0.1$  g) OPE mass, and  $W_{MD}$  (g) MD mass.

### 2.4. Microcapsule analyses

#### 2.4.1. Moisture content and water-solubility

Microcapsules (0.5 g) were dried at  $105^{\circ}\text{C}$  for 24 h, and their moisture content ( $MC_M$ ) was determined based on mass loss by drying and expressed in g/100 g.

Microcapsule water solubility index ( $WS_M$ , %), was determined as follows. Microcapsules (0.2 g) were mixed with 2.4 mL of deionized water in vortex for 1 min, the resulting suspension was incubated in water bath at  $30^{\circ}\text{C}$  for 30 min and centrifuged at 2090g for 15 min, and the supernatant dried at  $105^{\circ}\text{C}$  for 24 h.  $WS_M$  was calculated as (Paini et al., 2015):

$$WS_M = \frac{DW_S}{DW_M} \times 100 \quad (2)$$

where  $DW_S$  (g) is the supernatant dry mass.

#### 2.4.2. Release of bioactive compounds from microcapsules

Total and surface bioactive compounds were extracted from microcapsules according to Robert et al. (2010) with some modifications. For total extraction (TE), approximately 0.2 g of microcapsules were mixed with 1.0 mL of methanol, 0.16 mL of acetic acid and 0.84 mL of deionized water and mixed in vortex for 1 min at room temperature. Microcapsules were then broken twice in an ultrasonic bath, model UTA 90 (FALC Instruments s.r.l., Treviglio, BG, Italy), for 20 min, and the mixture was centrifuged at  $17000 \times g$  for 10 min. Superficial

extraction (SE) was performed in the same way but using a 1:1 (v/v) ethanol/methanol solution, and the resulting dispersion filtered through membranes with 0.45 µm-pore diameter (Sartorius Stedim Biotech GmbH, Goettingen, Germany).

Specific TP content ( $TP_M$ ) of microcapsules, expressed in mg of caffeic acid equivalent (CAE) per g of dry microcapsules ( $mg_{CAE}/g_{DW}$ ), was determined as:

$$TP_M = \frac{TP_E \times V_E}{DW_M} \quad (3)$$

where  $TP_E$  is TP concentration ( $mg_{CAE}/mL_E$ ) in OPE obtained either by total extraction (TE) or superficial extraction (SE), and  $V_E$  OPE volume (2.0 mL).

Specific antioxidant activity of microcapsules ( $AA_M$ ,  $\mu g_{Trolox}/g_{DW}$ ) was determined as:

$$AA_M = \frac{AA_E \times V_E}{DW_M} \quad (4)$$

where  $AA_E$  is antioxidant activity of the extract obtained by TE ( $mg_{Trolox}/mL_{TE}$ ).

TP yield of microcapsules ( $Y_{TP}$ , %) containing the extract obtained either by TE or SE was defined as:

$$Y_{TP} = \frac{TP_M \times DW_M}{TP_E \times V_E} \times 100 \quad (5)$$

with  $V_E = 50$  mL.

TP encapsulation efficiency ( $EE_{TP}$ , %) was determined as the complement to 100% of  $Y_{TP}$  referred to SE.

#### 2.4.3. Scanning electron microscopy

Microcapsules prepared under optimal conditions were observed by scanning electron microscopy (SEM 515, Philips, Netherlands). Small amounts of powders were coated with a 30 nm-thick gold layer and observed in secondary electron images (25.0 kV) at  $500\times$  and  $1000\times$  magnifications.

#### 2.4.4. Stability tests

Microcapsules prepared under optimal conditions were stored either at room temperature (25 °C) under artificial light (62 W-lamp at 2.1 klx) or in fridge at around 1–4 °C for 56 days. During storage, microcapsules were kept in sealed Eppendorf tubes to avoid moisture interference. TP and antioxidant activity of TE extract were analyzed after different storage times.

#### 2.5. Analytical methods

TP were quantified by the Folin–Ciocalteu assay (Swain & Hillis, 1959). Aliquots of reaction mixture were submitted to optical density (OD) determination at 725 nm with a UV–Vis spectrophotometer, model Lambda 25 (Perkin Elmer, Wellesley, MA, USA), using caffeic acid as standard ( $OD_{725} = 0.002TP$ ;  $R^2 = 0.9962$ ). TP content of raw material was expressed in  $mg_{CAE}/g_{DW}$ , while that of OPE obtained either by TE or SE in  $mg_{CAE}/mL_E$ .

The antioxidant activity was quantified as described by Re et al. (1999) with some modifications, using Trolox as antioxidant standard. The ABTS radical cation ( $ABTS^{\cdot+}$ ) was produced by reaction of an ABTS stock solution with 2.42 mM potassium persulfate and allowing the mixture to stand in the dark at room temperature for 12–16 h before use. After addition of 1.0 mL of diluted  $ABTS^{\cdot+}$  solution ( $OD_{734nm} = 0.74 \pm 0.02$ ) to 50 µL of sample, OD at 734 nm was read at room temperature 2 min after initial mixing and up to 3 min. The activity was standardized against standard methanolic solutions of Trolox in the range 0–0.8  $mg_{Trolox}/L$  using  $OD_{734nm} = -0.3364 C_{Trolox} + 0.6239$  ( $R^2 = 0.997$ ) and expressed in  $mg_{Trolox}/g_{DW}$  or  $mg_{Trolox}/mL_E$ .

The main free phenolic compounds, namely tyrosol, syringic acid,

caffeic acid, ferulic acid, oleuropein, and apigenin were identified by a high-performance liquid chromatograph, model 1100 (Agilent, Palo Alto, CA, USA), using a UV detector (at 280 nm) and a C18 reverse-phase column, model 201TP54 (Vydac, Hesperia, CA, USA), with a C18 guard column (Alltech Associates Inc., Deerfield, IL, USA), as described by Aliakbarian et al. (2011) and Painsi et al. (2016). Prior to injection, samples were filtered through 0.20 µm membranes (Sartorius Stedim Biotech GmbH, Goettingen, Germany). The injection volume was 100 µL. Two solvents were used as mobile phase: solvent A (1.0% acetic acid in water, v/v) and solvent B (50% methanol, 50% acetonitrile, v/v). A linear gradient was run at 30 °C with flow rate of 1 mL/min from 5% to 30% B in 25 min, from 30% to 40% B in 10 min, from 40% to 48% B in 5 min, from 48% to 70% B in 10 min, from 70% to 100% B in 5 min, isocratic at 100% B for 5 min, followed by returning to the initial conditions (10 min) and column equilibration (12 min). The concentration of each phenolic compound was calculated based on its standard solutions and the results were expressed in  $mg/100 g_{DW}$ .

#### 2.6. RSM and ANN modeling

RSM combined with a Central Composite Face Centered (CCFC) design was used as a former optimization approach. Experimental results of olive pomace extract microencapsulation carried out according to the CCFC design are listed in Table 2. The influence of IT, MD concentration, FF and AF, selected as independent variables, on six responses, namely  $Y_M$ ,  $MC_M$ ,  $WS_M$ ,  $TP_M$ ,  $AA_M$ , and  $EE_{TP}$ , was described by polynomial models. Central point was repeated three times to estimate the experimental error and check the suitability of models, while the Fisher's test for analysis of variance (ANOVA) was applied to evaluate their statistical significance. Statistically non-significant terms ( $p > 0.1$ ) were omitted in models. The “Design Expert” software, trial version 7.0.0 (Stat-Ease, Minneapolis, MN, USA), was employed for the regression analysis and numerical optimization.

Results were also modeled according to the multi-layer perception feed-forward Artificial Neural Network (ANN), trained as described by Aghbashlo, Mobli, Rafiee, and Madadlou (2013) and Sampaio et al. (2016). The WEKA software (Witten & Frank, 2005), version 3.6.0, was chosen to generate ANN models. For this purpose, two different network architectures were obtained using two training methods, namely 10-fold cross-validation and training/test. Proposed ANNs consisted of three kinds of layers: i) input layer with four neurons related to the independent variables, ii) hidden layer (default and 10–20 layers) with two neurons for each layer, a sigmoid transfer function between hidden layers, a linear transfer function between the last hidden layer and the output layer, and, finally, iii) output layer with a neuron associated with the responses. The epochs' number and momentum ranged from 500 to 20,000 and from 0.1 to 0.2, respectively, the learning rate was 0.5, and the default set in WEKA software was used for all other parameters. ANN models were optimized through the same genetic algorithm to obtain a Pareto-Front. RSM and ANN models' performances were statistically evaluated in terms of determination coefficient ( $R^2$ ) and mean square error (MSE).

### 3. Results and discussion

#### 3.1. Olive pomace extraction

Average TP concentration in six OPE ( $56 \pm 7 mg_{CAE}/g_{DW}$ ) and concentrations of the main phenolics, namely tyrosol ( $\cong 40.0 mg/100 g_{DW}$ ), syringic acid ( $\cong 3.7 mg/100 g_{DW}$ ), caffeic acid ( $\cong 3.7 mg/100 g_{DW}$ ), ferulic acid ( $\cong 3.0 mg/100 g_{DW}$ ), oleuropein ( $\cong 270 mg/100 g_{DW}$ ) and apigenin ( $\cong 7.0 mg/100 g_{DW}$ ), were very close to those reported by Painsi et al. (2015) and Painsi et al. (2016) for the same raw material using a similar extraction protocol. These results confirm the repeatability of extraction procedure using different olive pomace batches. OPE-TP, which proved stable at fridge temperature for up to 28 days

**Table 2**

Experimental results of olive pomace extract microencapsulation by spray drying carried out according to the Central Composite Face Centered design.

Run	Independent variable <sup>a</sup>				Responses					
	$x_1$	$x_2$	$x_3$	$x_4$	$Y_M^b$ (%)	$MC_M^c$ (%)	$WS_M^d$ (%)	$TP_M^e$ (mg <sub>CAE</sub> /g <sub>DM</sub> )	$AA_M^f$ (μg <sub>Trolox</sub> /g <sub>DM</sub> )	$EE_{TP}^g$ (%)
1	-1	+1	+1	+1	61	22	65	11	20	83.6
2	-1	0	0	0	56	14	69	25	172	87.9
3	-1	-1	-1	-1	62	7	77	38	293	76.6
4	-1	-1	+1	-1	44	10	80	47	293	61.0
5	-1	+1	-1	+1	69	22	75	10	47	80.7
6	0	0	+1	0	65	18	79	31	48	86.8
7	0	0	0	+1	81	12	74	17	37	77.8
8	0	+1	0	0	69	14	72	11	25	86.8
9	0	0	0	0	80	13	82	21	174	84.2
10	0	0	-1	0	78	14	77	17	28	64.3
11	0	0	0	0	78	12	79	20	174	84.9
12	0	-1	0	0	79	15	71	55	337	83.2
13	0	0	0	0	82	18	75	25	187	84.5
14	0	0	0	-1	51	17	81	21	166	86.0
15	+1	-1	+1	+1	74	11	81	38	36	91.6
16	+1	+1	+1	-1	51	22	75	11	47	85.5
17	+1	0	0	0	78	13	77	15	13	79.8
18	+1	+1	-1	-1	39	20	67	20	122	86.8
19	+1	-1	-1	+1	78	10	65	56	345	75.8
CP Mean <sup>h</sup>	0	0	0	0	80 ± 2	14 ± 3	79 ± 3	22 ± 3	178 ± 7	84.5 ± 0.3

<sup>a</sup> According to Table 1.<sup>b</sup>  $Y_M$  = microencapsulation yield.<sup>c</sup>  $MC_M$  = moisture content of microcapsules.<sup>d</sup>  $WS_M$  = water solubility of microcapsules.<sup>e</sup>  $TP_M$  = specific total polyphenol content of microcapsules.<sup>f</sup>  $AA_M$  = specific antioxidant activity of microcapsules.<sup>g</sup>  $EE_{TP}$  = total polyphenol encapsulation efficiency.<sup>h</sup> CP Mean = Mean values ± standard deviation at the central point (runs 9, 11 and 13).

(results not shown), were subsequently microencapsulated by spray drying using maltodextrin as carrier.

### 3.2. Microencapsulation of bioactive compounds

Varying the selected four independent variables, we obtained from OPE 19 powders by spray drying according to the CCFC design detailed in Table 2, which also lists the results of responses. Microencapsulation yield ranged from 39 to 82%, microcapsules moisture content from 7 to 22 g/100 g, their water solubility from 65 to 82%, specific TP content from 10 to 56 mg<sub>CAE</sub>/g<sub>DM</sub>, specific antioxidant activity of total bioactive compounds from 13 to 345 μg<sub>Trolox</sub>/g<sub>DM</sub>, and TP encapsulation efficiency from 61.0 to 91.6%. Paini et al. (2015), without performing any optimization of OPE microencapsulation by spray drying, observed lower values of  $MC_M$  (2.1–7.0 g/100 g) and  $TP_M$  (4.4–39.5 mg<sub>CAE</sub>/g<sub>DM</sub>) but almost coincident values of  $WS_M$  (79–87%) and  $EE_{TP}$  (51–94%).

The highest  $Y_M$  values (runs 7, 9 and 13) were obtained at intermediate values of IT, MD and FF,  $TP_M$  (runs 4, 12 and 19) and  $AA_M$  (runs 3, 4, 12 and 19) were maximized and  $MC_M$  was minimized (runs 3, 4 and 19) at the lowest MD concentrations, whereas  $WS_M$  and  $EE_{TP}$  did not show any regular trend. In their attempt to encapsulate with MD polyphenol-rich extract from *Averrhoa carambola* pomace, Saikia, Mahnot, and Mahanta (2015) observed a  $EE_{TP}$  increase from 63 to 79%, while  $WS_M$  kept almost constant (43–45%), when MD concentration was raised from 10 to 20 g/L. Mishra, Kumar Rai, and Mahanta (2015) reported for lemon juice powder no influence of MD concentration or IT on  $WS_M$  (94–98%), while  $AA_M$  was affected by an increase in both variables, likely due to the adverse impact of high temperature on phenolics structure and the MD dilution effect.

### 3.3. RSM approach

RSM was applied to optimize the responses considering linear, quadratic and interaction effects among independent variables. Table 3

**Table 3**

Analysis of variance (ANOVA) of data of significant responses of olive pomace extract microencapsulation by spray drying performed according to the Central Composite Face Centered design.

Response <sup>a</sup>	ANOVA				
	Source	SS <sup>b</sup>	DF <sup>c</sup>	F-value	p-value <sup>d</sup>
$Y_M$	Model	3112.2	9	17.1	0.0001
	Residual	181.99	9		
	Lack of fit	173.16	7	5.6	0.1598
	Pure error	8.83	2		
	Total	3294.19	18		
$MC_M$	Model	312.14	5	21.53	< 0.0001
	Residual	37.69	13		
	Lack of fit	21.40	11	0.24	0.9555
	Pure error	16.29	2		
	Total	349.83	18		
$TP_M$	Model	3424.57	5	23.33	< 0.0001
	Residual	381.63	13		
	Lack of fit	367.70	11	4.80	0.1849
	Pure error	13.93	2		
	Total	3806.1	18		

<sup>a</sup>  $Y_M$  = microencapsulation yield,  $MC_M$  = moisture content of microcapsules and  $TP_M$  = specific total polyphenol content of microcapsules.<sup>b</sup> SS = sum of squares.<sup>c</sup> DF = degree of freedom.<sup>d</sup> Statistically significant values < 0.1.

lists the results of ANOVA applied only to the three responses ( $Y_M$ ,  $MC_M$  and  $TP_M$ ) whose models were significant at 90% confidence level ( $p < 0.1$ ) and that exhibited insignificant lack of fit ( $p > 0.1$ ) relative to pure error; however, the pure error was low, indicating good data reproducibility. The corresponding coded second-order polynomial models with statistically significant terms ( $p < 0.1$ ) and those kept to



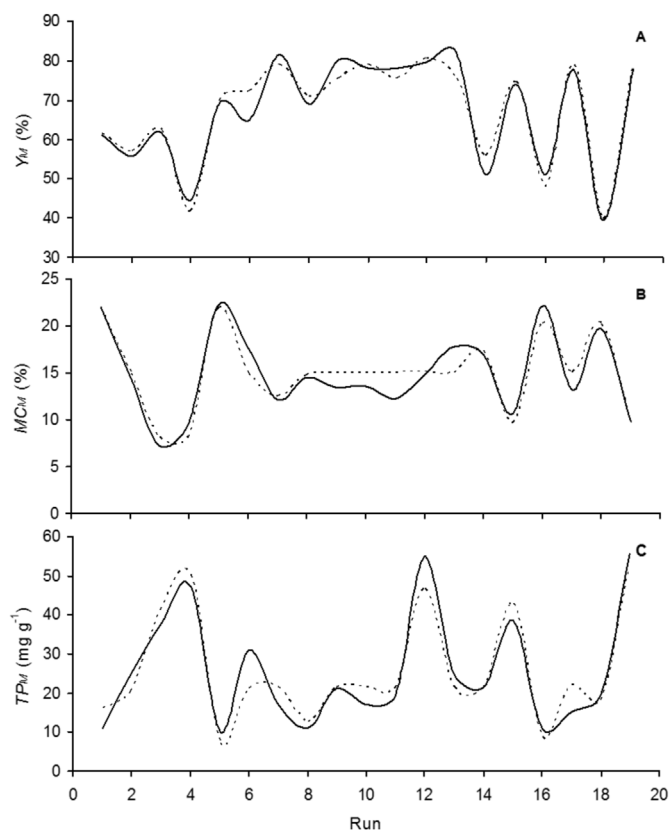


Fig. 1. Experimental values (—) and values predicted by Response Surface Methodology models (.....) of (A) yield of olive pomace microencapsulation by spray drying ( $Y_M$ ), (B) moisture content of microcapsules ( $MC_M$ ) and (C) specific total polyphenol content of microcapsules ( $TP_M$ ). Run conditions are detailed in Tables 1 and 2.

respect hierarchy were:

$$Y_M = 75.70 + 11.04 x_1 - 4.76 x_2 - 3.16 x_3 + 11.63 x_4 + 4.14 x_1 x_3 + 3.05 x_2 x_3 + 10.34 x_2 x_4 - 7.72 x_1^2 - 8.40 x_4^2 \quad (6)$$

$$MC_M = 14.96 + 0.01 x_1 - 0.2 x_4 - 3.22 x_1 x_2 - 6.28 x_1 x_4 \quad (7)$$

$$TP_M = 21.32 + 0.92 x_1 - 17.08 x_2 - 0.16 x_3 - 4.56 x_1 x_3 + 8.39 x_2^2 \quad (8)$$

where  $x_1$ ,  $x_2$ ,  $x_3$  and  $x_4$  are coded levels of IT, MD concentration, FF and AF, respectively.

Eq. (6) shows negative linear effects of  $x_2$  and  $x_3$  and positive ones of  $x_1$  and  $x_4$  on  $Y_M$ , while quadratic negative effects were exerted only by  $x_1$  and  $x_4$ , and those of two-way interactions  $x_1 x_3$ ,  $x_2 x_3$  and  $x_2 x_4$  were positive. One can see in Eq. (7) positive and negative linear effects of  $x_1$  and  $x_4$  on  $MC_M$ , respectively, a negative effect of  $x_1 x_2$  and  $x_1 x_4$ , but no significant contribution of  $x_3$ . Finally, Eq. (8) reveals a linear positive effect of  $x_1$  on  $TP_M$ , linear negative effects of  $x_2$  and  $x_3$ , a negative effect of  $x_1 x_3$  and a positive quadratic one of  $x_2$ , but no significant  $x_4$  contribution.

Fig. 1 shows good correlation between the results of these three responses (solid lines) and those predicted by RSM models (dotted lines).  $R^2$  ranged from 0.892 to 0.945 and MSE from 1.98 to 20.08 (Table 4), which means that the above models showed good predictive ability.

Models obtained for the other responses ( $WS_M$ ,  $AA_M$  and  $EE_{TP}$ ) were not significant ( $p > 0.1$ ) (results not shown), likely because modeling of spray drying microencapsulation is influenced by several factors, among which liquid atomization, rapid heat and mass transfer, curst formation, intensive solvent evaporation, complex segregation inside the generated, complex flow pattern (Aghbashlo et al., 2013). For this reason, these responses were alternatively modeled by ANN using two

Table 4  
Statistical parameters of response modeling by Response Surface Methodology and Artificial Neural Network applied to olive pomace microencapsulation by spray drying.

Parameter	RSM models			ANN models		
	$Y_M^a$	$MC_M^b$	$TP_M^c$	$WS_M^d$	$AA_M^e$	$EE_{TP}^f$
Determination coefficient ( $R^2$ )	0.945	0.892	0.900	0–1	0.5–1	0–1
Mean square error (MSE)	9.53	1.98	20.08	0–5.2	0–129.0	0–17.7

<sup>a</sup>  $Y_M$  = microencapsulation yield.

<sup>b</sup>  $MC_M$  = moisture content of microcapsules.

<sup>c</sup>  $TP_M$  = specific total polyphenol content of microcapsules.

<sup>d</sup>  $WS_M$  = water solubility of microcapsules.

<sup>e</sup>  $AA_M$  = specific antioxidant activity of microcapsules.

<sup>f</sup>  $EE_{TP}$  = total polyphenol encapsulation efficiency.

different training methodologies.

### 3.4. ANN approach

Six ANN architectures were tested for  $WS_M$ ,  $AA_M$  and  $EE_{TP}$ , varying the number of hidden layers, epoch's number and momentum.  $R^2$  and MSE varied from 0 to 1.0 and from 0 to 129.0, respectively (Table 4), with the highest and lowest  $R^2$  values obtained by training/test and cross-validation training, respectively. As stressed by Sampaio et al. (2016), the former training methodology deliberately overtrains the network, which justifies so high  $R^2$  values. Conversely, the so low  $R^2$  values obtained by cross validation ( $\leq 0.5$ ) demonstrate the impossibility to obtain a network, probably due to the small number of inputs (16 runs).

$R^2$  values close to unity do not always imply adequacy of a model (Sampaio et al., 2016); therefore, ANNs were used to predict the three responses from unseen input data (Table 5). In the case of Test A, referring to mean values at the central point, the predicted  $AA_M$  value was more than 10% lower than the experimental one, whereas those of  $WS_M$  and  $EE_{TP}$  were practically coincident with them. In that of Test B, an additional run differing from those used in the CCFC design, the experimental values of  $WS_M$  and  $EE_{TP}$  were approximately 4 and 25% higher than the predicted ones, respectively, while those of  $AA_M$  coincident. It can be inferred that networks had sufficient predictive capacity from unknown data, ensuring satisfactory convergence between predicted and experimental values.

### 3.5. Optimization with RSM and ANN models

With the aim of definitively identifying the optimal conditions for OPE microencapsulation, numeric and graphic optimizations were conducted using the Design Expert software for RSM models and the WEKA one for ANNs models to set the Pareto-Front. The former methodology essentially consists of overlaying the curves of RSM models for  $Y_M$ ,  $MC_M$  and  $TP_M$ , according to the specific criteria imposed, i.e., maximizing  $Y_M$  and  $TP_M$ , and minimizing  $MC_M$ . Thirty optimal numerical values representing a region of optimal responses were generated, the ranges of whose independent variables and responses are listed in Table 6. According to this approach, the best performance in terms of  $Y_M$  (65–82%),  $MC_M$  (9–14 g/100 g) and  $TP_M$  (38–52 mg<sub>CAE</sub>/g<sub>DW</sub>) was achieved when IT, MD concentration, FF and AF varied in the ranges 132–160 °C, 100–130 g/L, 5.0–10.0 mL/min and 26–32 m<sup>3</sup>/h, respectively.

Contour plots of  $Y_M$ ,  $MC_M$  and  $TP_M$  RSM models are depicted in Fig. 2. At the two lowest values of FF (5.0 and 7.5 mL/min) and AF (20 and 26 m<sup>3</sup>/h),  $Y_M$  increased with lowering MD concentration and raising IT (panels A1 and A2), whereas at the highest ones  $Y_M$  increased with increasing both MD and IT (panel A3). As a result, a simultaneous increase in the four independent variables led to the highest  $Y_M$  value

**Table 5**

Results of response prediction by Artificial Neural Network from unseen input data applied to olive pomace microencapsulation by spray drying.

Validation	Independent variable				Response					
					Experimental			Predicted		
	IT <sup>a</sup> (°C)	MD <sup>b</sup> (g/L)	FF <sup>c</sup> (mL/min)	AF <sup>d</sup> (m <sup>3</sup> /h)	WS <sub>M</sub> <sup>e</sup> (%)	AA <sub>M</sub> <sup>f</sup> (mg/g)	EE <sub>TP</sub> <sup>g</sup> (%)	WS <sub>M</sub> <sup>e</sup> (%)	AA <sub>M</sub> <sup>f</sup> (μg <sub>Trolox</sub> /g <sub>DM</sub> )	EE <sub>TP</sub> <sup>g</sup> (%)
Test A <sup>h</sup>	145	300	7.5	26	79 ± 3	180 ± 9	84.5 ± 0.4	74–77	74–112	64.4–84.6
Test B <sup>i</sup>	151	100	5.0	27	75 ± 1	303 ± 34	97.8 ± 0.2	66–69	304–342	69.4–72.1

<sup>a</sup> IT = inlet temperature.<sup>b</sup> MD = maltodextrin concentration.<sup>c</sup> FF = feed flowrate.<sup>d</sup> AF = air flowrate.<sup>e</sup> WS<sub>M</sub> = water solubility of microcapsules.<sup>f</sup> AA<sub>M</sub> = specific antioxidant activity of microcapsules.<sup>g</sup> EE<sub>TP</sub> = total polyphenol encapsulation efficiency.<sup>h</sup> Mean value at the central point.<sup>i</sup> Additional microencapsulation test carried out under conditions other than those of runs listed in Table 2.

(86%, panel A3). Likewise, Tee, Luqman Chuah, Pin, Abdull Rashih, and Yusof (2012) observed, for *Piper betle* L. leaves extract coated with maltodextrin, a  $Y_M$  increase with simultaneously raising IT and AF; but, contrary to what was observed in the present study,  $Y_M$  decreased with increasing FF.

Conversely, the simultaneous decrease of MD concentration and IT led, at the lowest FF and AF values, to a decrease in  $MC_M$  (10%, Fig. 2, panel B1), whereas exactly the opposite occurred at the highest levels of the same variables (7%, panel B3). At intermediate FF and AF values, any increase in one of these variables associated with a decrease of the other negatively impacted on this response (panel B2). As a result, the lowest  $MC_M$  values (< 7 g/100 g) were observed at the highest levels of the independent variables. Encapsulating the polyphenolic extract from *A. carambola* pomace with MD, Saikia et al. (2015) observed a  $MC_M$  decrease with increasing MD, and Mishra et al. (2015) reported a  $MC_M$  reduction during lemon juice powder spray drying when increasing MD concentration and IT. The same effect of IT and MD was observed by Selvamuthukumar and Khanum (2014) for spray drying of fruit juice slurry powder, while Tee et al. (2012) observed for *Piper betle* L. leaves extract coated with MD a  $MC_M$  decrease with increasing IT and AF.

Finally, a decrease of MD concentration, irrespectively of IT, FF and AF, enabled to maximize  $TP_M$  that reached a maximum value of 42 mg<sub>CAE</sub>/g<sub>DM</sub> (Fig. 2, panel C). At the lowest FF and AF levels (panels C1 and C2), an increase in MD concentration and a simultaneous decrease of IT led to a reduction of this response to 10 and 13 mg<sub>CAE</sub>/g<sub>DM</sub>, respectively. Similar trends were observed for spray drying of lemon juice (Mishra et al., 2015), likely due to thermal degradation of phenolics, *Morinda citrifolia* L. fruit extract (Krishnaiah, Bono, Sarbatly, Nithyanandam, & Anisuzzaman, 2015) and polyphenol-rich extract

from *A. carambola* pomace (Saikia et al., 2015).

RSM models' ability to predict response optimal values was checked through a confirmation test (Table 6). Experimental  $Y_M$  and  $TP_M$  values were within the ranges presented in graphical/numerical optimization, while that of  $MC_M$  was 4 g/100 g higher compared with the predicted value (9–14 g/100 g). These results demonstrate satisfactory convergence between predicted numerical optimization and experimental values of the confirmation test.

For ANN models, a multiple-objective optimization using genetic algorithms was performed, since the objectives were conflicting ( $AA_M$  and  $EE_{TP}$  maximization, and  $WS_M$  minimization). Pareto-Front solutions were observed at 100 g/L MD varying IT, FF and AF in the ranges 146–151 °C, 5–8 mL/min and 31–36 m<sup>3</sup>/h, respectively, conditions under which  $WS_M$ ,  $AA_M$  and  $EE_{TP}$  varied in the ranges 64–65%, 230–487 μg<sub>Trolox</sub>/g<sub>DM</sub> and 85–92%, respectively (results not shown). Test B, whose results are listed in Table 5, was taken as a confirmation test in the optimal region obtained in the Pareto-Front for  $WS_M$ ,  $AA_M$  and  $EE_{TP}$ .  $AA_M$  experimental value (303 ± 34 μg<sub>Trolox</sub>/g<sub>DM</sub>) was within the range of predicted values (230–487 μg<sub>Trolox</sub>/g<sub>DM</sub>), while those of  $WS_M$  (75 ± 1%) and  $EE_{TP}$  (97.8 ± 0.2%) were 13% and 6% higher than the predicted ones. In general, satisfactory convergence was observed between predicted Pareto-Front and experimental values of Test B.

Ranges of optimization by ANN models (IT = 146–151 °C, MD = 100 g/L, FF = 5–8 mL/min and AF = 31–32 m<sup>3</sup>/h) were close to those obtained by RSM ones (IT = 132–160 °C, MD = 100–130 g/L, FF = 5–10 mL/min and AF = 26–32 m<sup>3</sup>/h), which means that the two optimizations converged to the same region for the selected responses.

**Table 6**

Numerical optimization by overlaying response surface plots and experimental results of confirmation test of olive pomace microencapsulation by spray drying.

	Independent variable				Response		
	IT <sup>a</sup> (°C)	MD <sup>b</sup> (g/L)	FF <sup>c</sup> (mL/min)	AF <sup>d</sup> (m <sup>3</sup> /h)	$Y_M$ <sup>e</sup> (%)	$MC_M$ <sup>f</sup> (%)	$TP_M$ <sup>g</sup> (mg <sub>CAE</sub> /g <sub>DM</sub> )
Optimization	132–160	100–130	5–10	26–32	65–82	9–14	38–52
Confirmation test <sup>h</sup>	151	100	5	27	73 ± 0	14 ± 0	52 ± 5

<sup>a</sup> IT = inlet temperature.<sup>b</sup> MD = maltodextrin concentration.<sup>c</sup> FF = feed flowrate.<sup>d</sup> AF = air flowrate.<sup>e</sup>  $Y_M$  = microencapsulation yield.<sup>f</sup>  $MC_M$  = moisture content of microcapsules.<sup>g</sup>  $TP_M$  = specific total polyphenol content of microcapsules.<sup>h</sup> Test B of Table 5.

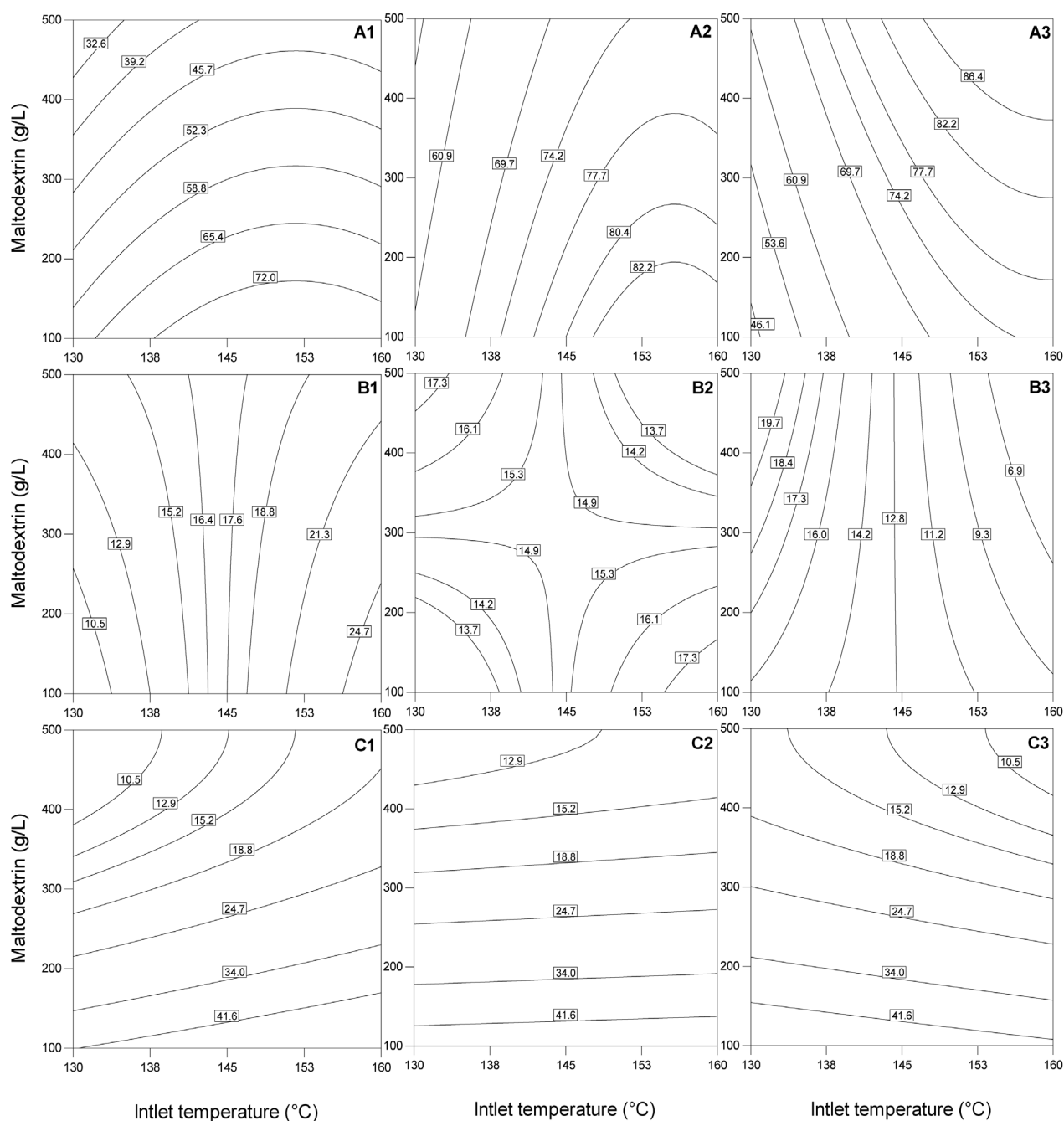


Fig. 2. Contour plots for optimization by Response Surface Methodology models of (A) yield of olive pomace microencapsulation by spray drying, (B) moisture content of microcapsules and (C) specific total polyphenol content of microcapsules. (1) feed flowrate (FF) = 5.0 mL/min, air flowrate (AF) = 20 m<sup>3</sup>/h; (2) FF = 7.5 mL/min, AF = 26 m<sup>3</sup>/h; (3) FF = 10.0 mL/min, AF = 32 m<sup>3</sup>/h. Values within rectangles correspond to those of the respective response.

### 3.6. Scanning electron microscopy and microcapsule stability

Scanning electron microscopy observations of maltodextrin and microcapsules obtained through the confirmation test (Table 6) are illustrated in Fig. 3. MD micrographs revealed spherical particles due to powder aggregation and amorphous structures (panels A and B), while those of microcapsules (panels C and D) relatively-polydisperse spherical structure with smooth surface, confirming the observations of Painei et al. (2015). Damages occurred in a few microcapsules (arrows in panels C and D) indicated that they were hollow. Microparticle diameter measured from the image ranged approximately from 2 to 25  $\mu\text{m}$ .

To simulate storage conditions of microcapsules for possible industrial applications, they were submitted to 56 days-long stability tests at room temperature under artificial light or at 1–4  $^{\circ}\text{C}$  in the dark.

Almost irrespective of light and temperature, microcapsules showed  $TP_M$  and  $AA_M$  values 12 and 9% lower, respectively, than the initial sample (results not shown), suggesting that both conditions would be suitable for long storage. These results confirm those of Painei et al. (2015) who observed 7.5–15% decreases of the same responses.

## 4. Conclusions

Olive pomace extract was successfully encapsulated in maltodextrin microcapsules by spray drying for the first time. First, a comprehensive optimization study has been done using either Response Surface Methodology or Artificial Neural Network. The same optimization regions for operative parameters were obtained using these two statistical approaches. However, the results indicated that the prediction accuracy

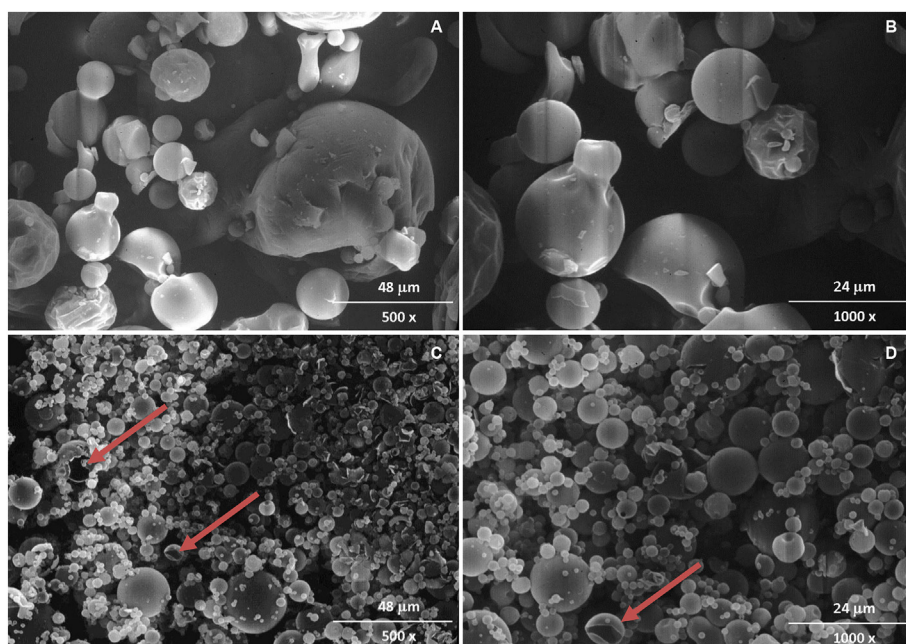


**Fig. 3.** Scanning electron microscopy images: (A) pure maltodextrin at 500 ×; (B) pure maltodextrin at 1000 ×; (C) olive pomace-containing microcapsules at 500 ×; (D) olive pomace-containing microcapsules at 1000 ×. Microcapsules were obtained by spray drying at 151 °C inlet temperature, 100 g/L maltodextrin concentration, 5 mL/min<sup>-1</sup> feed flowrate and 27 m<sup>3</sup>/h air flowrate. The arrows show the damage that is atypical for this sample.

of RSM was better than that of ANN. Optimal microencapsulation conditions were met when inlet temperature, maltodextrin concentration, feed flowrate and air flowrate were in the ranges 132–160 °C, 100–160 g/L, 5.0–10.0 mL/min and 26–32 m<sup>3</sup>/h, respectively. Microscopic observation of microcapsules obtained under optimal conditions revealed that they were spherical particles with smooth surface and had average diameter in the range 5–25 μm. The most important finding of this study is that microcapsules showed high recovery of polyphenols, remarkable antioxidant activity and good stability under storage conditions, which suggests their possible exploitation in functional food and pharmaceutical products.

### Acknowledgment

The authors thank Brazilian CNPq for the post-doc fellowship of Dr. F.C. Sampaio.

### References

- Aghbashlo, M., Mobli, H., Rafiee, S., & Madadlou, A. (2013). An artificial neural network for predicting the physicochemical properties of fish oil microcapsules obtained by spray drying. *Food Science and Biotechnology*, 22, 677–685.
- Akhavan Mahdavi, S., Jafari, S. M., Assadpoor, E., & Dehnad, D. (2016). Microencapsulation optimization of natural anthocyanins with maltodextrin, gum Arabic and gelatin. *International Journal of Biological Macromolecules*, 85, 379–385.
- Aliakbarian, B., Casazza, A. A., & Perego, P. (2011). Valorization of olive oil solid waste using high pressure-high temperature reactor. *Food Chemistry*, 128, 704–710.
- Aliakbarian, B., De Faveri, D., Converti, A., & Perego, P. (2008). Optimisation of olive oil extraction by means of enzyme processing aids using response surface methodology. *Biochemical Engineering Journal*, 42(1), 34–40.
- Aliakbarian, B., Palmieri, D., Casazza, A. A., Palombo, D., & Perego, P. (2012). Antioxidant activity and biological evaluation of olive pomace extract. *Natural Product Research*, 26, 2280–2290.
- Barbanera, M., Lascaro, E., Stanzione, V., Esposito, A., Altieri, R., & Bufacchi, M. (2016). Characterization of pellets from mixing olive pomace and olive tree pruning. *Renewable Energy*, 88, 185–191.
- Casazza, A. A., Aliakbarian, B., De Faveri, D., Fiori, L., & Perego, P. (2012). Antioxidants from winemaking wastes: A study on extraction parameters using response surface methodology. *Journal of Food Biochemistry*, 36(1), 28–37.
- Castro, N., Durrieu, V., Raynaud, C., & Rouilly, A. (2016). Influence of DE-value on the physicochemical properties of maltodextrin for melt extrusion processes. *Carbohydrate Polymers*, 144, 464–473.
- Christoforou, E., & Fokaidis, P. A. (2016). A review of olive mill solid wastes to energy utilization techniques. *Waste Management*, 49, 346–363.
- Desai, K. G. H., & Park, H. J. (2005). Recent developments in microencapsulation of food ingredients. *Drying Technology*, 23, 1361–1394.
- Edris, A. E., Kalembe, D., Adamiec, J., & Piątkowski, M. (2016). Microencapsulation of

- Nigella sativa* oleoresin by spray drying for food and nutraceutical applications. *Food Chemistry*, 204, 326–333.
- Gabbay Alves, T. V., Silva da Costa, R., Aliakbarian, B., Casazza, A. A., Perego, P., et al. (2017). Microencapsulation of *Theobroma cacao* L. waste extract: Optimization using response surface methodology. *Journal of Microencapsulation*, 34(2), 111–120.
- Hojjati, M., Razavi, S. H., Rezaei, K., & Gilani, K. (2011). Spray drying microencapsulation of natural canthaxanthin using soluble soybean polysaccharide as a carrier. *Food Science and Biotechnology*, 20, 63–69.
- Huang, S. M., Kuo, C. H., Chen, C. A., Liu, Y. C., & Shieh, C. J. (2017). RSM and ANN modeling-based optimization approach for the development of ultrasound-assisted liposome encapsulation of piceid. *Ultrasonics Sonochemistry*, 36, 112–122.
- Kalogeropoulos, N., Kaliora, A. C., Artemiou, A., & Giogios, I. (2014). Composition, volatile profiles and functional properties of virgin olive oils produced by two-phase vs three-phase centrifugal decanters. *LWT-Food Science and Technology*, 58, 272–279.
- Klen, T. J., Wondra, A. G., Vrhovšek, U., & Vodopivec, B. M. (2015). Phenolic profiling of olives and olive oil process-derived matrices using UPLC-DAD-ESI-QTOF-HRMS analysis. *Journal of Agricultural and Food Chemistry*, 63, 3859–3872.
- Krishnaiah, D., Bono, A., Sarbaty, R., Nithyanandam, R., & Anisuzzaman, S. M. (2015). Optimisation of spray drying operating conditions of *Morinda citrifolia* L. fruit extract using response surface methodology. *Journal of King Saud University-Engineering Sciences*, 27, 26–36.
- Mishra, P., Kumar Rai, G., & Mahanta, C. (2015). Process standardization for development of spray-dried lemon juice powder and optimization of Amla-lemon based RTS (ready-to-serve) drink using response surface methodology. *Journal of Food Processing and Preservation*, 39, 1216–1228.
- Paini, M., Aliakbarian, B., Casazza, A. A., Lagazzo, A., Botter, R., & Perego, P. (2015). Microencapsulation of phenolic compounds from olive pomace using spray drying: A study of operative parameters. *LWT-Food Science and Technology*, 62, 177–186.
- Paini, M., Casazza, A. A., Aliakbarian, B., Perego, P., Binello, A., & Cravotto, G. (2016). Influence of ethanol/water ratio in ultrasound and high-pressure/high-temperature phenolic compound extraction from agri-food waste. *International Journal of Food Science and Technology*, 51, 349–358.
- Poshadri, A., & Aparna, K. (2010). Microencapsulation technology: A review. *Journal of Research Angra*, 38, 86–102.
- Re, R., Pellegrini, N., Proteggente, A., Pannala, A., Yang, M., & Rice-Evans, C. (1999). Antioxidant activity applying an improved ABTS radical cation decolorization assay. *Free Radical Biology & Medicine*, 26, 1231–1237.
- Robert, P., Goren, T., Romero, N., Sepulveda, E., Chavez, J., & Saenz, C. (2010). Encapsulation of polyphenols and anthocyanins from pomegranate (*Punica granatum*) by spray drying. *International Journal of Food Science and Technology*, 45, 1386–1394.
- Saikia, S., Mahnot, N. K., & Mahanta, C. L. (2015). Optimisation of phenolic extraction from *Averrhoa carambola* pomace by response surface methodology and its microencapsulation by spray and freeze drying. *Food Chemistry*, 171, 144–152.
- Sampaio, F. C., Saraiva, T. L. C., de Lima e Silva, G. D., Faria, J. T., Pitangui, C. G., Aliakbarian, B., et al. (2016). Batch growth of *Kluyveromyces lactis* cells from de-proteinized whey: Response surface methodology versus Artificial neural network – genetic algorithm approach. *Biochemical Engineering Journal*, 109, 305–311.
- Selvamuthukumar, M., & Khanum, F. (2014). Optimization of spray drying process for developing seabuckthorn fruit juice powder using response surface methodology. *Journal of Food Science & Technology*, 51, 3731–3739.
- Swain, T., & Hillis, W. E. (1959). The phenolic constituents of *Prunus domestica*. The quantitative analysis of phenolic constituents. *Journal of the Science of Food and Agriculture*, 10, 63–68.



- Tee, L. H., Luqman Chuah, A., Pin, K. Y., Abdull Rashih, A., & Yusof, Y. A. (2012). Optimization of spray drying process parameters of *Piper betle* L. (Sirih) leaves extract coated with maltodextrin. *Journal of Chemical and Pharmaceutical Research*, 4, 1833–1841.
- Witten, I. H., & Frank, E. (2005). *Data mining: Practical machine learning tools and techniques* (2nd ed.). San Francisco, CA: Morgan Kaufmann Publishers.
- Wyspiańska, D., Kucharska, A. Z., Sokół-Łętowska, A., & Kolniak-Ostek, J. (2016). Physicochemical, antioxidant, and anti-inflammatory properties and stability of hawthorn (*Crataegus monogyna* Jacq.) procyanidins microcapsules with inulin and maltodextrin. *Journal of the Science of Food and Agriculture*, 97, 669–678.
- Zhang, C., Li, X., Liu, Y. N., & Zhang, F. (2015). Utilization of microcapsule technology in foods. *Journal of Nanoscience and Nanotechnology*, 15, 9330–9340.
- Zuidam, N. J., & Shimoni, E. (2010). Overview of microencapsulates for use in food products or processes and methods to make them. In N. Zuidam, & V. Nedovic (Eds.). *Encapsulation technologies for active food ingredients and food processing* (pp. 3–29). New York, NY: Springer.